Severity of Neurodegeneration Correlates with Compromise of Iron Metabolism in Mice with Iron Regulatory Protein Deficiencies

SOPHIA R. SMITH,[a] SHARON COOPERMAN,[a] TIM LAVAUTE,[a,b] NANCY TRESSER,[c] MANIK GHOSH,[a] ESTHER MEYRON-HOLTZ,[a] WILLIAM LAND,[a] HAYDEN OLLIVIERRE,[a] BERNARD JORTNER,[d] ROBERT SWITZER III,[e] ALBEE MESSING,[f] AND TRACEY A. ROUAULT[a,g]

[a]*National Institute of Child Health and Human Development, Cell Biology and Metabolism Branch, Bethesda, Maryland, USA*

[d]*Laboratory for Neurotoxicity Studies, Virginia Tech, Blacksburg, Virginia, USA*

[e]*NeuroScience Associates, Knoxville, Tennessee, USA*

[f]*Department of Pathobiological Sciences and Waisman Center, University of Wisconsin-Madison, Madison, Wisconsin, USA*

ABSTRACT: In mammals, iron regulatory proteins 1 and 2 (IRP1 and IRP2) posttranscriptionally regulate expression of several iron metabolism proteins including ferritin and transferrin receptor. Genetically engineered mice that lack IRP2, but have the normal complement of IRP1, develop adult-onset neurodegenerative disease associated with inappropriately high expression of ferritin in degenerating neurons. Here, we report that mice that are homozygous for a targeted deletion of IRP2 and heterozygous for a targeted deletion of IRP1 (IRP1+/– IRP2–/–) develop a much more severe form of neurodegeneration, characterized by widespread axonopathy and eventually by subtle vacuolization in several areas, particularly in the substantia nigra. Axonopathy develops in white matter tracts in which marked increases in ferric iron and ferritin expression are detected. Axonal degeneration is significant and widespread before evidence for abnormalities or loss of neuronal cell bodies can be detected. Ultimately, neuronal cell bodies degenerate in the substantia nigra and some other vulnerable areas, microglia are activated, and vacuoles appear. Mice manifest gait and motor impairment at stages when axonopathy is pronounced, but neuronal cell body loss is minimal. These observations suggest that therapeutic strategies that aim to revitalize neurons by treatment with neurotrophic factors may be of value in IRP2–/– and IRP1+/– IRP2–/– mouse models of neurodegeneration.

KEYWORDS: iron; neurodegeneration; IRP; substantia nigra; axonopathy; ferritin

[b]Present address: Tim LaVaute, University of Wisconsin, Madison, WI.

[c]Formerly of Neuroimmunology Branch, National Institute of Neurologic Disease and Stroke, Bethesda, MD.

[g]Address for correspondence: Dr. Tracey A. Rouault, NIH/NICHD/CBMB, Building 18T, Room 101, Bethesda, MD 20892. Voice: 301-496-7060; fax: 301-402-0078.
trou@helix.nih.gov

Ann. N.Y. Acad. Sci. 1012: 65–83 (2004).
doi: 10.1196/annals.1306.006

Iron is an essential element for function of the central nervous system since it participates in a variety of critical metabolic processes including oxygen transport, electron transport, and DNA synthesis. In the CNS, iron is required for biosynthesis of several neurotransmitters[1,2] and for the function of numerous enzymes required for oxidative phosphorylation, including iron-sulfur proteins and cytochromes. In normal animals, iron reproducibly accumulates in characteristic brain areas as animals mature.[3]

Accumulation of excess iron is hypothesized to play a role in pathogenesis of some neurodegenerative diseases. Increased iron has frequently been noted in brain regions that develop pathology in common diseases such as Parkinson's disease[4] and Alzheimer's disease,[5] as well as in rare conditions such as NBIA 1 disease (neuronal brain iron accumulation type 1, formerly known as Hallervorden-Spatz syndrome),[6] autosomal recessive juvenile parkinsonism,[7] multiple systems atrophy,[8] and Friedreich's ataxia.[9]

Recently, we reported that genetic ablation of iron regulatory protein 2 (IRP2−/−) in mice results in misregulation of iron metabolism in several tissues and is associated with adult-onset neurodegenerative disease.[10] IRP2 is one of two iron regulatory proteins (IRPs) responsible for regulation of iron homeostasis in mammalian cells (reviewed in refs. 11 and 12). Both IRPs are cytosolic proteins that bind to RNA stem-loop motifs known as IREs found in the 5′ UTR of ferritin H and L subunit transcripts, in the 3′ UTR of the transferrin receptor (TfR), and in several other iron metabolism gene transcripts. Each of the two IRPs, IRP1 and IRP2, binds to IREs when cells are depleted of iron. When IRPs bind to ferritin transcripts, they interfere with translation and decrease synthesis of ferritin protein; in contrast, when they bind to the TfR transcript, they protect the mRNA from degradation, leading to increased synthesis of TfR. The two IRPs are 58% homologous in sequence, but they have different mechanisms for sensing iron levels.[11,12]

Although both IRPs are expressed in the central nervous system, neurodegenerative disease does not develop in IRP1−/− animals (Meyron-Holtz *et al*., *EMBO J*., in press). The unexpected absence of a neurological phenotype in IRP1−/− mice raised the possibility that IRP1 does not contribute to posttranscriptional regulation of iron metabolism in the brain. However, here we report that animals that lack both copies of IRP2 and one copy of IRP1 (IRP1+/− IRP2−/−) develop a form of neurodegenerative disease that is much more severe than that of IRP1+/+ IRP2−/− mice. In these mice, additional loss of one IRP1 allele further compromises regulation of iron metabolism in several tissues including brain, indicating that IRP1 contributes to iron homeostasis in multiple tissues, but its role is apparent only when the mouse lacks sufficient IRP2 for regulation. In this report, we focus on characterizing the phenotype and pathology of IRP1+/− IRP2−/− mice, an important new animal model of adult-onset neurodegeneration.

MATERIALS AND METHODS

Targeted Deletion of IRP1 and IRP2

Embryonic stem cells were transfected with constructs, chimeric mice were bred, and Southern analyses were performed on mouse tail cuts as previously described.[10]

IRP1+/– IRP2–/– animals were bred by mating IRP1+/– IRP2+/– animals and genotyping offspring.

Chemistries and Blood Work

Serum chemistries and complete blood counts were performed by the Veterinary Research Pathology Branch of the NIH.

Serum ferritins were measured as previously described.[10]

Western Analysis of Mouse Tissues

Mouse tissues were minced in Triton buffer containing 25 mM Tris, 40 mM KCl, 0.1 mM DTT, 1 mM AEBSF, 10 μg/mL leupeptin, 1 tablet/50 mL complete, and 1% Triton. Homogenized tissues were quickly centrifuged to remove large debris. Protein concentrations were measured using Bradford assay. Equal amounts of proteins from the tissues of three different genotypes were loaded on a 13% SDS-PAGE (for ferritin) and an 8% gel (for TfR), and detection of ferritin and TfR was as previously described.[10]

Histopathology

Age- and sex-matched WT, IRP2–/–, and IRP1+/– IRP2+/– mice between the ages of 4 and 12 months were anesthetized with pentobarbital IP and transcardially perfused with 4% paraformaldehyde/PBS.[10] Tissues were removed by dissection and post-fixed for 24 h at 4°C, followed by embedding in gelatin and staining of sections using H&E, GFAP, Perls' DAB,[13] or amino-cupric silver stain[14] as previously described.[10] Alternatively, tissues of perfused animals were cryoprotected in 30% sucrose/PBS overnight. Forty-μm cryostat sections were processed for detection of microglial activation using rat anti-mouse Mac 1 antibody (1:200; Serotec) followed by biotinylated goat anti-rat Ig secondary antibody (1:200, Serotec).

Tyrosine hydroxylase immunohistochemistry was performed on paraffin-embedded sagittal sections of mice of each genotype using mouse anti-tyrosine hydroxylase antibodies (Zymed) at a final concentration of 1 μg/mL.

Ferritin immunohistochemistry was performed as previously described.[10]

For high-resolution light microscopy and transmission electron microscopy studies, deeply anesthetized animals were transcardially perfused with 4% paraformaldehyde and 0.2% glutaraldehyde. Multiple regions of brain and spinal cord were postfixed in osmium tetroxide, embedded in Polybed epoxy® resin, sectioned at 1-μm thickness, stained using toluidine blue and safranin, and examined by light microscopy. Selected tissue blocks from this material were used for ultrastructural analyses. These were thin-sectioned, with the sections mounted on copper grids and stained with lead citrate and uranyl acetate. These specimens were examined by transmission electron microscopy.

Forelimb and hindlimb grip strength was assessed by hang-test using a custom-made grip as previously described.[10] Statistical analysis was performed using an unpaired, Student's *t* test.

RESULTS

IRP1+/– IRP2–/– Animals Develop Early-Onset Neurodegeneration

We generated mice with the genotype IRP1+/– IRP2–/– through breeding and compared them to IRP2–/– and WT mice. The loss of one copy of IRP1 significantly worsened the neurodegeneration of IRP2–/– mice. Symptoms including failure to support the abdomen and slow uncoordinated gait were easily observed at 4 months of age in IRP1+/– IRP2–/– animals, whereas these symptoms did not appear until many months later in IRP2–/– mice. To assess the neurologic impairment quantitatively, we employed the hang-test, in which the length of time that a mouse can hang on to an inverted wire screen is measured.[10] Notably, at 1 year of age, the IRP1+/– IRP2–/– mice were able to hang on for only 10.7 ± 9.3 s (n = 17), whereas IRP2–/– mice could hang on for an average of 33.9 ± 25.1 s (n = 22) and WT mice could usually hang on for a full minute (57.1 ± 6.7 s) (n = 34).

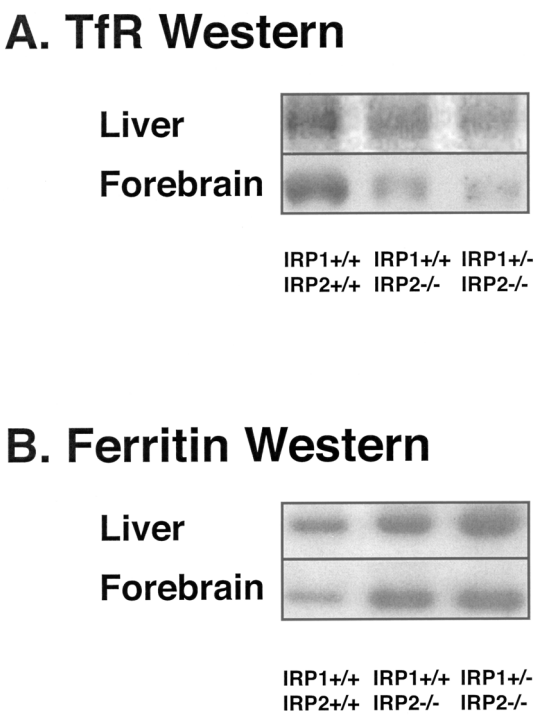

FIGURE 1. Misregulation of ferritin and TfR expression in tissues of WT, IRP2–/–, and IRP1+/– IRP2–/– mice. Total protein lysates were prepared from the mouse tissues indicated and subjected to Western analysis using the antibodies to TfR **(A)** and to ferritin **(B)**. Results shown are representative examples from experiments that have been performed on multiple mice of the indicated genotypes.

Ferritin and Transferrin Receptor Expression Are Abnormal in IRP1+/– IRP2–/– Mice

Since a major role of IRPs is to appropriately repress ferritin synthesis, we compared ferritin expression levels in lysates of multiple tissues from WT, IRP2–/–, and IRP1+/– IRP2–/– animals. Notably, ferritin levels in the forebrain and liver were higher in IRP1+/– IRP2–/– mice than in the IRP2–/– mice, indicating that loss of one IRP1 allele further impairs the compromised ability of IRP2–/– mice to repress ferritin translation (FIG. 1A). Serum ferritin was markedly increased in IRP1+/– IRP2–/– mice compared to IRP2–/– mice; serum ferritin of IRP1+/– IRP2–/– was 3000 ± 1900 ng/mL, whereas serum ferritin of IRP2–/– mice was 1800 ± 640 ng/mL, compared to WT serum ferritins of 740 ± 16 ng/mL. Transferrin receptor expression was decreased in the forebrain and liver of IRP2–/– and IRP1+/– IRP2–/– mice compared to WT (FIG. 1B), with slightly lower expression apparent in the IRP1+/– IRP2–/– mice.

To assess for compromise of tissue functions, we autopsied animals and evaluated histopathology of multiple tissues. In addition, we measured serum chemistries and complete blood counts of IRP1+/– IRP2–/– animals and WT animals. Despite abnormal iron metabolism in the liver, liver function tests including ALT, GST, LDH, and bilirubin were normal. BUN, a potential indicator of renal dysfunction, was also normal. Serum phosphorus was elevated in several IRP1+/– IRP2–/– animals that were agonal. The most noteworthy difference in blood work was that IRP1+/– IRP2–/– animals were anemic. Hemoglobin for WT animals was 13.32 ± 0.982 ($n = 6$), whereas serum hemoglobin was 9.86 ± 0.303 ($n = 6$, $p < .0005$). In addition, MCV was 50.35 ± 0.923 in WT vs. 38.1 ± 1.835, $p < .0005$. These values are consistent with an iron-deficiency anemia.

Ferric Iron Accumulation Colocalizes with Axonopathy in IRP2–/– and IRP1+/– IRP2–/– Mice

In order to examine pathology in the brain, we evaluated coronal sections of WT, IRP2–/–, and IRP1+/– IRP2–/– genotypes using the enhanced Perls' DAB stain for the detection of iron[13] and the amino-cupric silver stain[14] for the detection of axonal degeneration. As shown in FIGURES 2a–c, ferric iron accumulation in cerebellar white matter was substantially increased in IRP1+/– IRP2–/– mice compared to IRP2–/– animals. Moreover, comparable increases in silver impregnation of cerebellar white matter were seen in the IRP1+/– IRP2–/– animal compared to the IRP2–/– animal (FIGS. 2d–f).

Iron accumulation was observed in distinctive and reproducible regions of white and gray matter throughout the brain (summarized in TABLE 1). Usually when iron accumulation was observed in white matter tracts, evidence of axonal degeneration was also found, as evidenced by black threadlike areas of silver impregnation. Widespread axonal degeneration was also revealed throughout the brain by detection of myelin dense bodies characteristic of axonal degeneration, as illustrated in FIGURE 3. When iron accumulation was detected in gray matter areas such as the interpeduncular nucleus (FIG. 4) and mammillary body (not shown), there was rarely evidence of silver impregnation of cell bodies. However, when the projections of intact iron-laden neuronal cell bodies were examined, there was often evidence of axonal

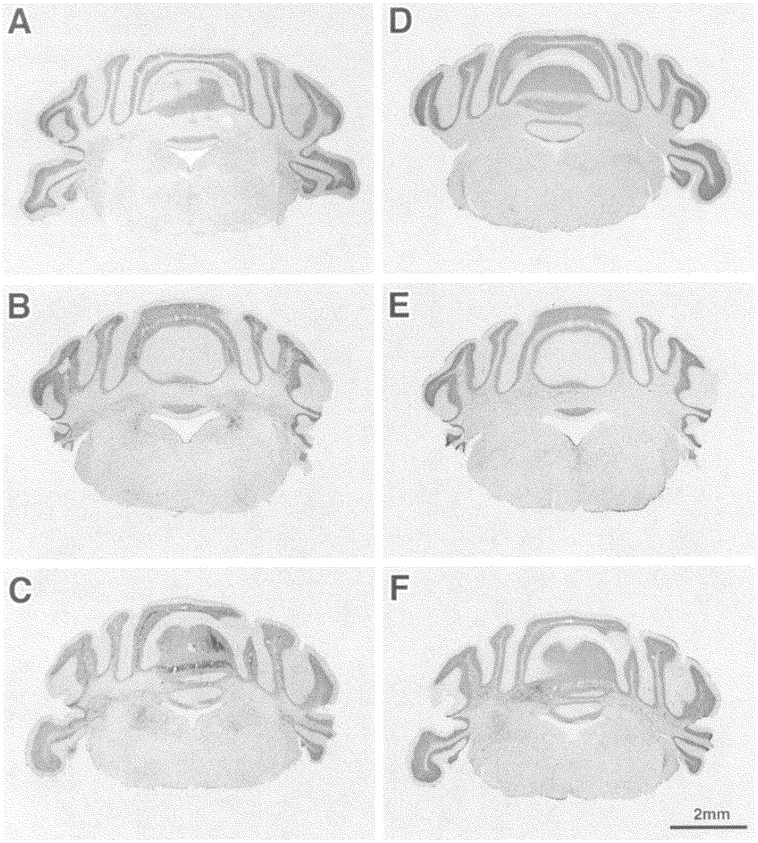

FIGURE 2. Iron accumulation and axonal degeneration colocalize and reveal an increase in axonal degeneration in the IRP1+/– IRP2–/– as compared to the WT **(A)** and IRP2–/– alone. In coronal sections through the metencephalon, ferric iron was detected as a brown precipitate with Perls' DAB stain in white matter of the IRP2–/– animal **(B)** and in the IRP1+/– IRP2–/– animal, where increased iron relative to the IRP2–/– animal was detected. Nuclei are counterstained with methyl green to show general morphology **(C)**. Silver impregnation indicative of axonal degeneration was prominent in areas that showed substantial iron accumulation, particularly at the tips of the cerebellar folia **(D–F)**. Nuclei are counterstained with neutral red to show morphology. [Figure shown in black and white.]

degeneration. For example, the mammillothalamic tract projects from cell bodies in the mammillary body that are heavily laden with iron, but silver does not impregnate the cell bodies and is discernible only in axons. When the time course of disease development was analyzed by comparing 4-, 9-, 12-, and 28-month-old mice, iron accumulation in white matter tracts preceded evidence of silver degeneration (data not shown).

TABLE 1. Iron accumulation in discrete tracts and nuclei of the brain correlates with areas of degeneration detected by the amino-cupric silver degeneration stain

Region	Enhanced Prussian Blue	Amino cupric
Telencephalon		
Anterior commissure	++	+
Caudate-putamen	+++	++
Hippocampus	++	++
Corpus callosum	-	-
Frontal cortex	-	-
CN II	+	+++
Diencephalon		
Fasciculus retroflexus	+++	-
Mamillary body	++	-
Mamillothalamic tract	-	++
Fornix	+++	+
Thalamus	++	++
Medial lemniscus	++	++
Medial longitudinal fasciculus	++	++
Posterior commissure	++	-
Mesencephalon		
Inferior and superior colliculi	+++	+++
Substantia nigra	++	++
CN III	+	+
CN IV	+	+
Interpeduncular nucleus	+++	-
Superior cerebellar peduncle	++	++
Nigrostriatal tract	++	+++
Metencephalon		
Cerebellum	+++	+++
Middle cerebellar peduncle	++	++
Inferior cerebellar peduncle	++	++
CN V	+	+
CN VI	+	+
CN VII	+	+
CN VIII	++	+
Myencephalon		
Nucleus gracilis	++	++

NOTE: Tracts in which significant iron staining was observed were evaluated to assess the corresponding level of silver impregnation, and conversely those with significant silver impregnation were examined for presence of iron. The nigrostriatal and cerebellar white matter tract silver impregnation was most intense and was used as the standard for +++ staining. The intense iron staining of the caudate putamen and cerebellar white matter was used as the standard for +++ iron staining. + was used to reflect faint, but clearly detectable iron staining or silver impregnation, and ++ was used to reflect easily detected silver or iron staining. As indicated, numerous areas of the brain were iron-loaded and showed silver impregnation. However, some areas including frontal cortex, internal capsule, and corpus callosum were completely spared.

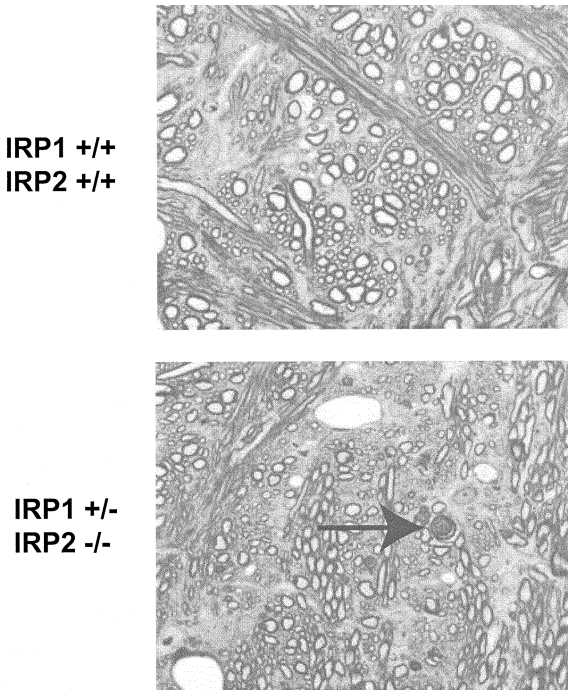

FIGURE 3. Axonopathy is also manifested by widespread presence of myelin dense bodies. Myelin dense bodies were detected throughout the brain of IRP1+/– IRP2–/– mice, but not in WT mice. Sections through the pons of epoxy-embedded, toluidine blue–stained brains of WT (*top*) and IRP1+/– IRP2–/– animals (*bottom*) are shown. Numerous myelin dense bodies are present, the largest of which is marked with an *arrow.*

Iron Overload, Degeneration, and Vacuolization Occur in the Substantia Nigra

The substantia nigra was very iron-rich in IRP2–/– and IRP1+/– IRP2–/– mice (FIG. 5a; left-hand panel) compared to WT controls. In addition, the nigrostriatal tract showed impressive silver degeneration, and some silver impregnation was detected in cell bodies in the substantia nigra pars compacta (SNPC) of IRP2–/– and IRP1+/– IRP2–/– mice (not shown). Careful morphologic evaluation of the SNPC on toluidine blue–stained sections of epoxy-embedded brains revealed that neuronal cell bodies were misshapen (FIG. 5a; right-hand panel). There was blebbing of the plasma membrane, loss of integrity of the nuclear membrane, and formation of numerous vacuoles ranging in size from approximately 5 to 50 microns in diameter that were most markedly increased in the IRP1+/– IRP2–/– mice. In FIGURE 5a, several typical vacuoles filled with debris are seen. In some instances, neuronal remnants were identifiable in these vacuoles, which we have previously detected in IRP2–/– mice using MRI.[15] Notably, although TUNEL assays were negative, assays

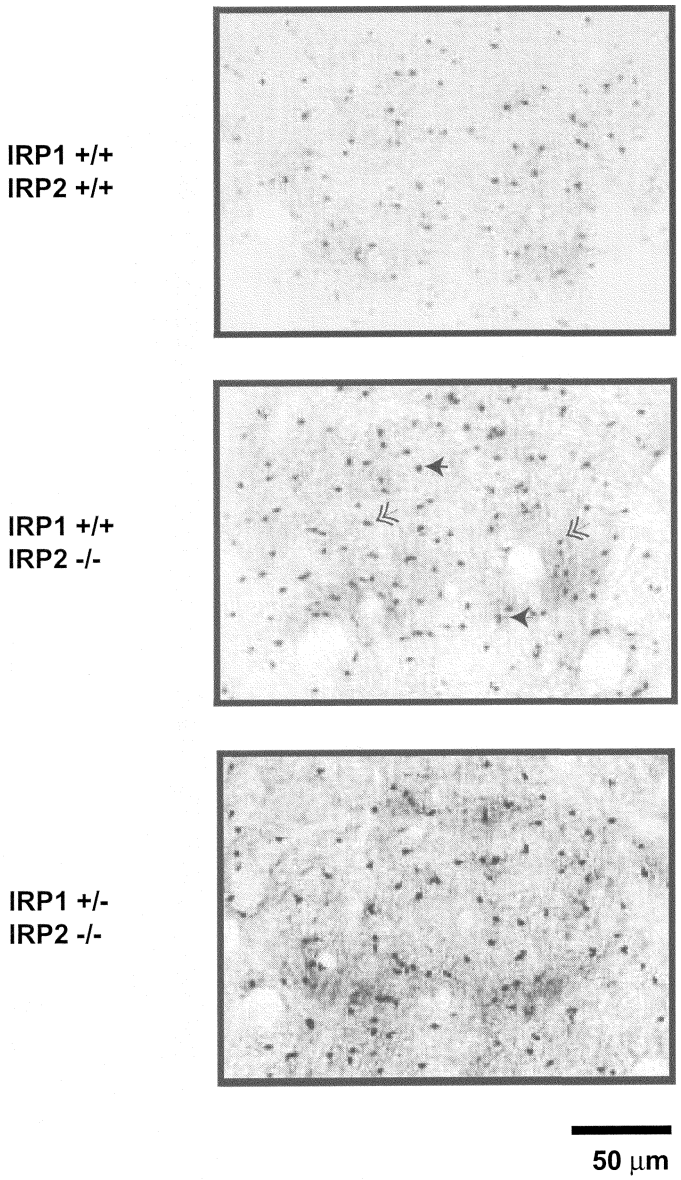

FIGURE 4. Iron accumulates in neuronal cell bodies and oligodendrocytes of the interpeduncular nucleus. Iron accumulation detected by Perls' DAB stain is present in neuronal cell bodies (*solid arrow*), oligodendrocytes (*double arrow*), and their processes. Iron accumulation is markedly increased in IRP1+/– IRP2–/– mice compared to IRP2–/– and to WT.

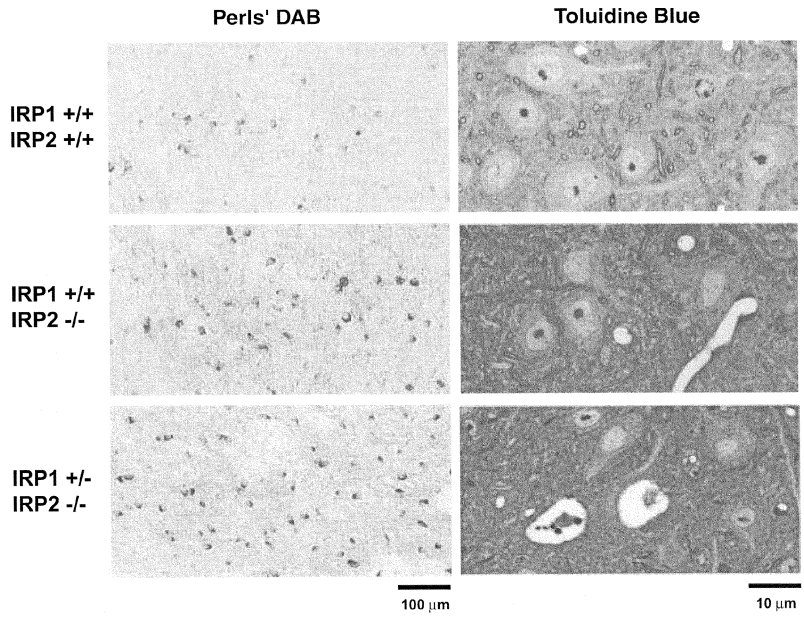

FIGURE 5a. Iron accumulation in the substantia nigra correlates with neuronal degeneration and the appearance of vacuolation. Iron accumulation is greatest in the substantia nigra of IRP1+/– IRP2–/– mice. Neurons of abnormal size and shape are detectable in substantia nigra of toluidine blue stains of epoxy-embedded brains in IRP2–/– mice, and more markedly in IRP1+/– IRP2–/– mice. Several characteristic vacuoles that contain debris are present in the IRP1+/– IRP2–/– toluidine blue stain.

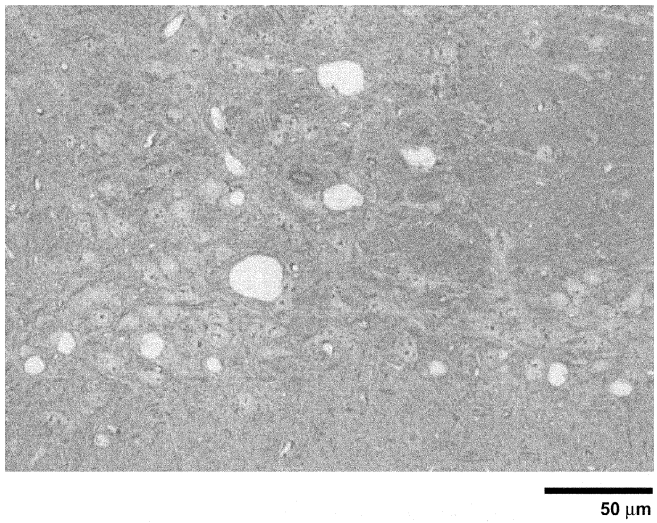

FIGURE 5b. A low-power view of the substantia nigra pars compacta of IRP1+/– IRP2–/– reveals multiple vacuoles ranging up to 30 μm in diameter. Many of the vacuoles are the approximate size of neuronal cell bodies.

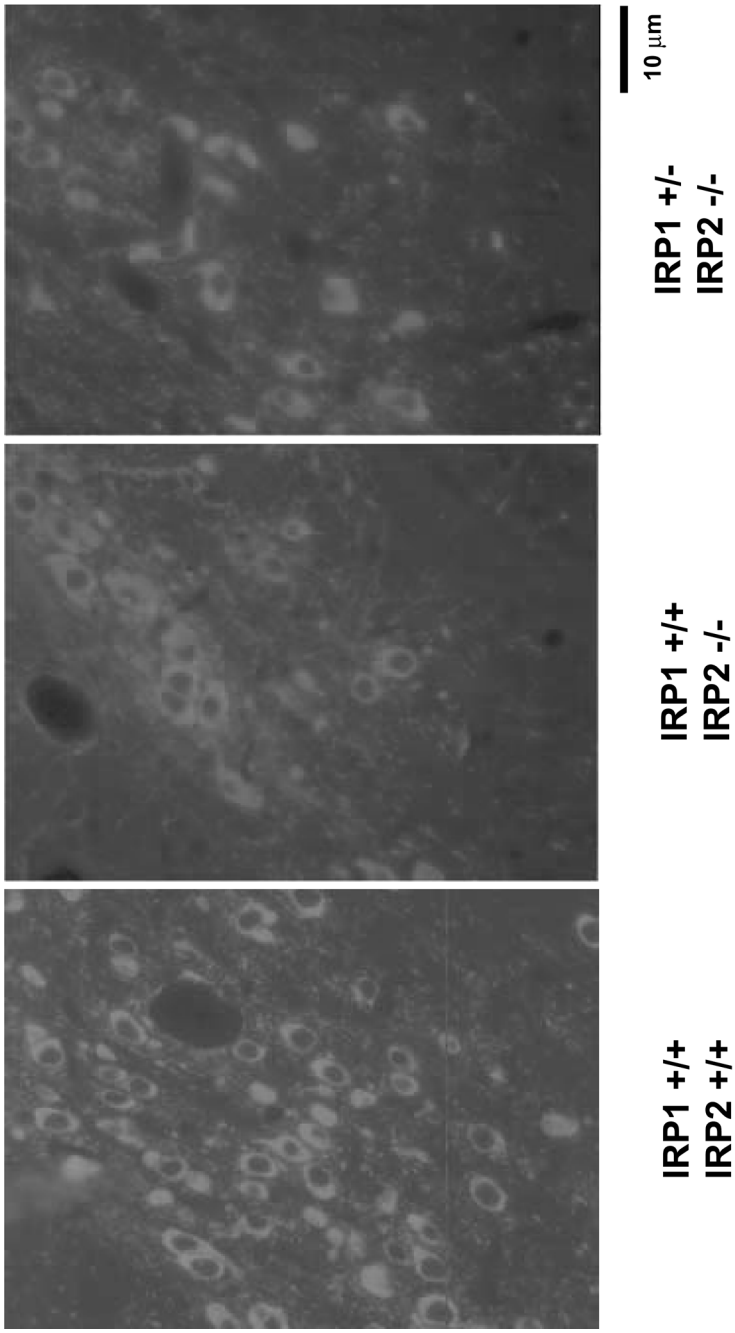

FIGURE 6. Decreased numbers of tyrosine hydroxylase–positive cells are detected in IRP2−/− and IRP1+/− IRP2−/− mice. Multiple sagittal sections were stained for tyrosine hydroxylase as described in MATERIALS AND METHODS and matched for anatomical location. Fewer tyrosine hydroxylase–positive cells were consistently detected in IRP2−/− and IRP1+/− IRP2−/− mice.

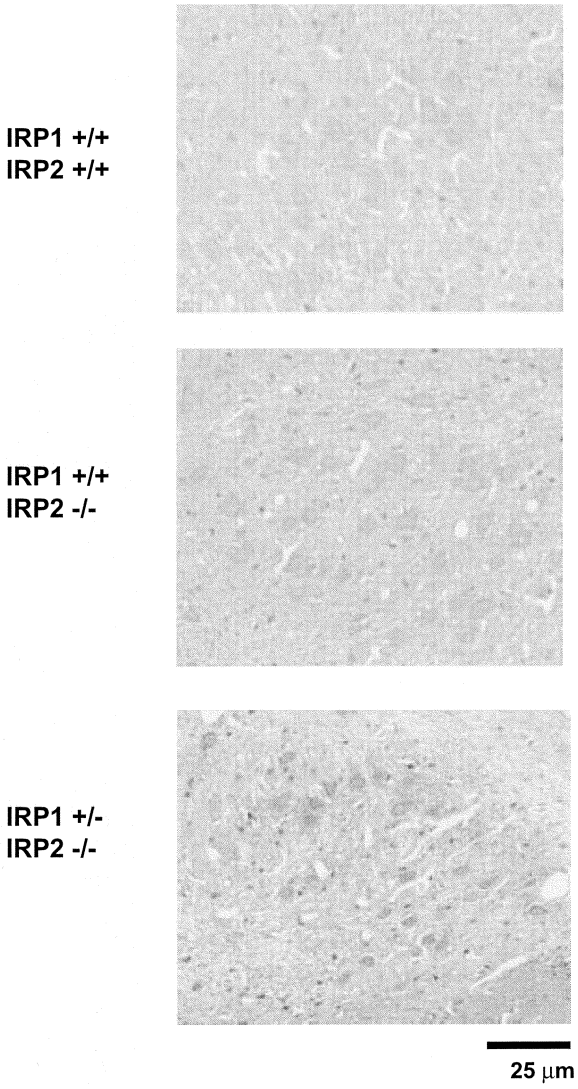

FIGURE 7. Increased ferritin is detected in neuronal cell bodies in the deep cerebellar nuclei of IRP2−/− and IRP1+/− IRP2−/− mice. Perfused and paraffin-embedded sagittal brain sections were stained with ferritin antibody as described in MATERIALS AND METHODS. Increased ferritin expression compared to WT was noted in the neuronal cell bodies in multiple brain areas (see TABLE 1). Shown here is increased ferritin expression in the deep cerebellar nuclei of IRP2−/− mice, a finding that was even more pronounced in the IRP1+/− IRP2−/− mice.

for activation of caspase III were lightly positive in the substantia nigra and in several other regions of the brain (data not shown). We counted the vacuoles in the SNPC of WT vs. IRP2–/– vs. IRP1+/– IRP2–/– mice and discovered that vacuole formation was much more pronounced in the IRP1+/– IRP2–/– mice than in the IRP2–/– mice, yielding a spongiform appearance in low-power views of the SN (FIG. 5b). In three 9-month-old IRP1+/– IRP2–/– mice, we counted an average of 17.8 ± 5.1 vacuoles per single section of SN; in contrast, in two age- and sex-matched IRP2–/– mice, we counted 8.5 ± 2.5 vacuoles per SN, and comparable vacuoles were not detected in two similarly processed age- and sex-matched WT

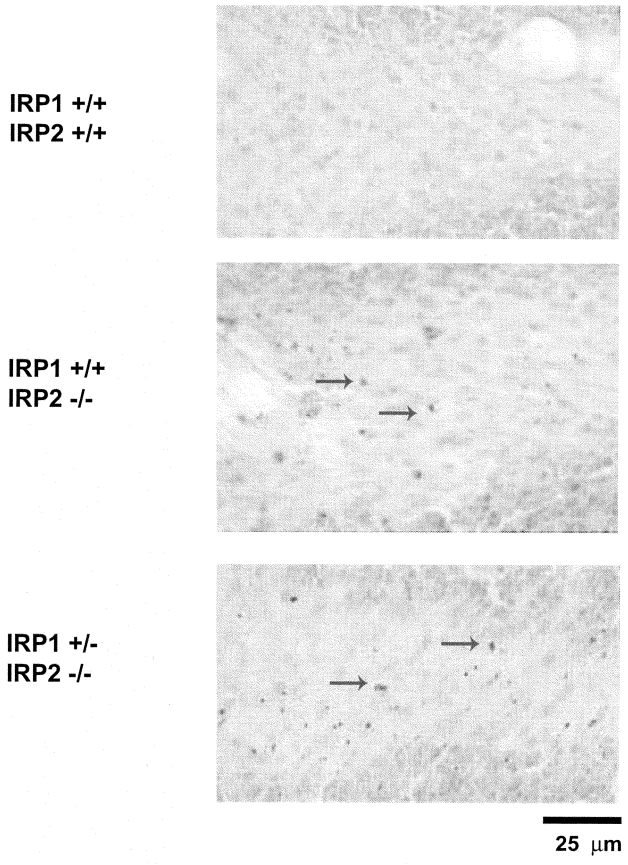

FIGURE 8. Markedly increased numbers of ubiquitin inclusions are present in cerebellar white matter of IRP1+/– IRP2–/– compared to IRP2–/– mice. Ubiquitin inclusions were detected in coronal sections of cerebellar white matter using anti-ubiquitin antibodies followed by avidin-biotin complex immunoperoxidase staining. Ubiquitin inclusions appear as intense brown spots (*arrows*), and nuclei of cerebellar granule cells are counterstained with methyl green (*appears as light gray in figure*).

mice. Immunohistochemistry for tyrosine hydroxylase confirmed that dopaminergic neurons were reduced in number in IRP1+/– IRP2–/– animals (FIG. 6).

Increased Ferritin Expression Is Detected within Neuronal Cell Bodies by Immunohistochemistry

In most areas that showed increased ferric iron, increased ferritin was detected by immunohistochemistry. Ferritin in neuronal cell bodies of the deep cerebellar nuclei increased markedly in IRP1+/– IRP2–/– mice compared to IRP2–/– animals, as

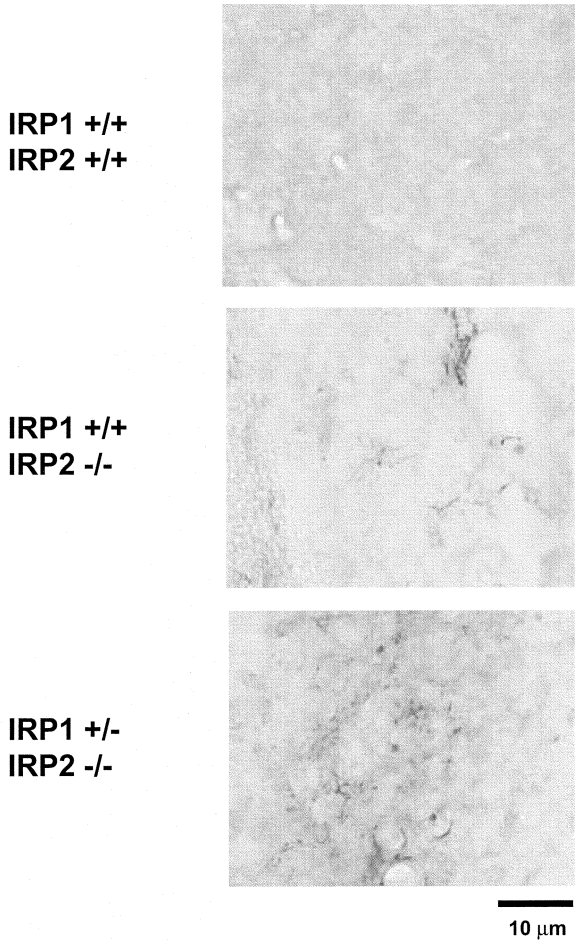

FIGURE 9. Foci of activated microglia are detected in IRP2–/– and IRP1+/– IRP2–/– mice. Using antibodies to activated microglia, frozen sections of brain were stained, and numerous activated microglia were found in IRP2–/– and IRP1+/– IRP2–/– mice.

indicated in FIGURE 7, and neuronal ferric iron increased comparably (data not shown). These observations are consistent with the interpretation that much of the increased ferric iron is sequestered within ferritin.[10]

Ubiquitin Inclusions Are Present in White Matter

A common feature of neurodegenerative diseases is the presence of ubiquitin-positive inclusions. Using anti-ubiquitin antibodies, we detected ubiquitin inclusions in IRP2–/– and IRP1+/– IRP2–/– mice. Notably, the number of ubiquitin inclusions in IRP1+/– IRP2–/– mice was markedly increased over the number found in IRP2–/– mice (FIG. 8).

Activated Microglia Are Prevalent in Brains of IRP2–/– and IRP1+/– IRP2–/– Animals

To pursue possible mechanisms that could lead to the formation of vacuoles observed in SNPC and to a lesser degree in the superior colliculus and pons (not shown), we looked for evidence of microglial or astroglial activation. Foci of activated microglia were found in some of the affected regions of the brain of IRP2–/– and IRP1+/– IRP2–/– mice. Activated microglia were distinctly increased in mice that were IRP1+/– IRP2–/– compared to mice that lacked IRP2 alone (FIG. 9). We did not find evidence for activation of astrocytes using the GFAP stain (not shown).

DISCUSSION

Mice with compromised iron regulatory protein function develop adult-onset neurodegenerative disease characterized by widespread axonopathy and later by vacuolization in discrete and reproducible areas of the brain, most prominently in the substantia nigra. The results of breeding between IRP1–/– and IRP2–/– mice indicate that IRP1 and IRP2 are partially redundant in function. Loss of one copy of IRP1 further exacerbates the neurodegenerative disease of IRP2–/– mice. This result is very interesting because IRP1–/– mice do not develop neurodegenerative disease, and we have discovered that IRP1 contributes minimally to normal iron regulation in WT mice (Meyron-Holtz *et al.*, submitted). The pronounced worsening of neurodegenerative disease in IRP1+/– IRP2–/– mice both clinically and pathologically compared to IRP2–/– mice correlates with increased compromise of the ability of cells in many tissues of IRP1+/– IRP2–/– mice to appropriately repress ferritin synthesis and increase stability of the transferrin receptor transcript.

In the central nervous system of IRP2–/– and IRP1+/– IRP2–/– mice, inappropriate ferritin expression is associated with ferric iron accumulation in discrete tracts and nuclei throughout the brain. Iron accumulation is substantial in numerous specific white matter tracts, where iron is present in invaginations of oligodendrocyte cytosol into the axonal space as well as in the axons themselves (Sheng *et al.*, in preparation). White matter tracts with significant iron accumulation degenerate, as indicated by the amino-cupric silver degeneration stain (FIG. 2) and presence of myelin dense

bodies detected in these regions on toluidine blue–stained epoxy-embedded tissue (FIG. 3). In contrast, silver impregnation generally spares most neuronal cell bodies. However, morphologic abnormalities can be detected in neuronal somata in several locations (FIGS. 5–7).[10] In the SN, neurons that accumulated iron and ferritin appeared to shrink, and occasionally the nucleolus could often be detected as a remnant in a developing vacuole (FIG. 5). Although the morphology of these pyknotic cells was not typical for apoptotic cells,[16] we found immunohistochemical evidence for activation of caspase III in the SN and to a lesser extent in several other locations. Therefore, the contribution of apoptosis to neurodegeneration is not yet clear.

In the SN, we found multiple vacuoles, many of which conformed to the size and shape of neuronal cell bodies. Using GFAP staining, we did not find a marked increase in astrocyte activity compared to WT controls. However, stains for activated microglia revealed multiple foci of activated microglia in regions of the brain that were degenerating. The presence of activated microglia may help to explain the genesis of the vacuoles in our mice. We suggest that microglia may remove remnants of shrunken pyknotic neurons and that absence of astroglial activation explains why vacuoles persist in affected regions of the brain. The degree of vacuolization is minimal compared to prion disease[17] and the recently described mahoganoid neurodegeneration model.[18] Thus, we have not yet discovered any good counterparts to our model in the literature. Electron microscopic analysis of these vacuoles indicates that these vacuoles are not membrane-bound, and the debris contents of the vacuole are not distinctive (not shown).

Our results do not yet allow us to determine why axonopathy develops in IRP2–/– and IRP1+/– IRP2–/– mice. The consequences of loss of IRP2 function include increased ferritin expression, decreased transferrin receptor expression,[10] and perhaps other as yet uncharacterized abnormalities in regulation of gene expression. We have previously proposed that axonal degeneration may be one of the earliest events in disease progression in IRP2–/– mice,[19] and our data support a similar interpretation for IRP1+/– IRP2–/– mice. The axonal degeneration takes place in tracts that are clearly loaded with ferritin and ferric iron. In white and gray matter areas that are iron-overloaded as judged by staining for ferric iron and ferritin, we find that oligodendrocytes are extremely loaded with ferritin iron (FIG. 3) and this includes not only the cytosol in the cell body of the oligodendrocyte, but also invaginations from the inner myelin sheath into the region of the axon (Sheng *et al*., in preparation). The fact that only those oligodendrocytes that are in close physical contact with iron-overloaded neurons develop ferritin iron overload could mean that the oligodendrocytes acquire iron from the adjacent neuronal cell body or axon. Notably, iron overload is not detected in oligodendrocytes of the frontal cortex, a region of the brain in which iron overload is not detected in neurons in our models. Since oligodendrocytes are generally regarded as a relatively homogeneous cell type, it seems most likely that the iron overload observed in distinct regions of the brain is secondary to some feature of the immediate environment. However, it will be important in the future to culture oligodendrocytes and various types of neurons from our animals to distinguish cells that are programmed to make primary errors in regulation of iron metabolism as a consequence of loss of IRP activity from those in which iron overload is determined by their location in the central nervous system.

Although overexpression of ferritin in our mouse models correlates well with development of neurodegeneration, these results conflict somewhat with those of a

recently reported study in which ferritin overexpression in the SN protected animals from the effects of MPTP injection.[20] However, it is also possible that our mice would be similarly protected from a single toxic insult from MPTP injection early in the course of disease. Similarly, it is possible that the transgenic mice that overexpress ferritin in the SN may have late-term pathology that has not yet been appreciated.

Although greater misregulation of ferritin and transferrin receptor expression is appreciable in multiple tissues of the IRP1+/– IRP2–/– mouse, it is interesting to note that the only systemic abnormality is an anemia in IRP1+/– IRP2–/– mice. We do not detect abnormalities of the liver (this paper), kidney (unpublished observations), and small intestine[10] as judged by serum tests and pathologic examination in IRP1+/– IRP2–/– mice, as was true for the IRP2–/– mice. These results underscore a conundrum that we previously encountered in IRP2–/– mice, namely that neurodegeneration occurs when other tissues affected by the same metabolic compromise exhibit normal function and histology. The subset of neurons that show evidence of misregulation of iron metabolism develop an axonopathy, whereas neurons in the cortex that do not accumulate iron and ferritin are spared.

It is not clear why some neurons are very adversely affected by a fundamental mistake in iron metabolism, whereas other tissues are spared. One possibility is that it takes time for damage to accrue, and injuries accumulate slowly in postmitotic neurons. However, vulnerability is unlikely to be determined solely by the expected life span of the cell; cardiomyocytes are also postmitotic cells, but there is no evidence for cardiomyocyte pathology in IRP2–/– or IRP1+/– IRP2–/– mice (not shown). Another possibility is that neurons are unusually vulnerable to mistakes in iron metabolism because they are highly polarized and iron redistributes to the axon and myelin sheath inappropriately in IRP2–/–[19] and IRP1+/– IRP2–/– mice (this paper).

A logical prediction from the observed exacerbation of misregulation of iron metabolism that occurs in IRP1+/– IRP2–/– mice is that IRP1–/– IRP2–/– mice would have an extremely severe form of neurodegenerative disease. However, we are unable to evaluate IRP1–/– IRP2–/– mice because complete loss of expression of both IRPs is embryonic lethal, with death occurring at the blastocyst stage (Smith and Rouault, in preparation). These results underscore our conclusion that both IRP1 and IRP2 contribute to normal posttranscriptional iron regulation in mammalian cells. IRP1–/– IRP2+/– animals look very similar to IRP1+/+ IRP2+/– animals[10] in that they have later-onset neurodegenerative disease that is less severe.

The presence in our mouse models of a pronounced axonopathy that is generally not associated with pathology and loss of neuronal cell bodies is interesting for studies of pathophysiology and therapeutics. In some instances, it is now recognized that axonopathy is preceded by nerve terminal injury.[21] A common form of axonopathy occurs in a process referred to as "dying back", but there is no evidence that dying back plays a role in our mice. Axonal degeneration that does not involve a classical "dying back" response has been described in association with axonal inclusions in motor neuron, Parkinson's, and Huntington's diseases.[22] If much of the disability of our mice results from compromised function of neurons that are alive, but impaired, as our models suggest, then therapeutic interventions could include delivery of neurotrophic factors such as NGF[22] or GDNF.[23] Neurotrophic factors could potentially revitalize function of impaired living neurons and reverse clinical symptomatology. IRP1+/– IRP2–/– mice may thus provide a model in which therapeutic interventions relevant to human disease can be tested.

ACKNOWLEDGMENTS

We thank the Veterinary Resources Program of the NIH for measuring complete blood counts and serum chemistries. This work was supported by the Intramural Program of the National Institute of Child Health and Human Development, with generous help from the Lookout Fund.

REFERENCES

1. PONTING, C.P. 2001. Domain homologues of dopamine beta-hydroxylase and ferric reductase: roles for iron metabolism in neurodegenerative disorders? Hum. Mol. Genet. **10:** 1853–1858.
2. CONNOR, J.R., G. PAVLICK, D. KARLI *et al*. 1995. A histochemical study of iron-positive cells in the developing rat brain. J. Comp. Neurol. **355:** 111–123.
3. HILL, J.M. & R.C. SWITZER III. 1984. The regional distribution and cellular localization of iron in the rat brain. Neuroscience **11:** 595–603.
4. BERG, D., M. GERLACH, M.B. YOUDIM *et al*. 2001. Brain iron pathways and their relevance to Parkinson's disease. J. Neurochem. **79:** 225–236.
5. SMITH, M.A., P.L. HARRIS, L.M. SAYRE & G. PERRY. 1997. Iron accumulation in Alzheimer disease is a source of redox-generated free radicals. Proc. Natl. Acad. Sci. USA **94:** 9866–9868.
6. HAYFLICK, S.J. 2003. Pantothenate kinase–associated neurodegeneration (formerly Hallervorden-Spatz syndrome). J. Neurol. Sci. **207:** 106–107.
7. TAKANASHI, M., H. MOCHIZUKI, K. YOKOMIZO *et al*. 2001. Iron accumulation in the substantia nigra of autosomal recessive juvenile parkinsonism. ARJP **7:** 311–314.
8. DICKSON, D.W., W. LIN, W.K. LIU & S.H. YEN. 1999. Multiple system atrophy: a sporadic synucleinopathy. Brain Pathol. **9:** 721–732.
9. WILSON, R.B. 2003. Frataxin and frataxin deficiency in Friedreich's ataxia. J. Neurol. Sci. **207:** 103–105.
10. LAVAUTE, T., S. SMITH, S. COOPERMAN *et al*. 2001. Targeted deletion of iron regulatory protein 2 causes misregulation of iron metabolism and neurodegenerative disease in mice. Nat. Genet. **27:** 209–214.
11. ROUAULT, T. & R. KLAUSNER. 1997. Regulation of iron metabolism in eukaryotes. Curr. Top. Cell. Regul. **35:** 1–19.
12. SCHNEIDER, B.D. & E.A. LEIBOLD. 2000. Regulation of mammalian iron homeostasis. Curr. Opin. Clin. Nutr. Metab. Care **3:** 267–273.
13. FRANCOIS, C., J. NGUYEN-LEGROS & G. PERCHERON. 1981. Topographical and cytological localization of iron in rat and monkey brains. Brain Res. **215:** 317–322.
14. DE OLMOS, J.S., C.A. BELTRAMINO & S. DE OLMOS DE LORENZO. 1994. Use of an amino-cupric-silver technique for the detection of early and semiacute neuronal degeneration caused by neurotoxicants, hypoxia, and physical trauma. Neurotoxicol. Teratol. **16:** 545–561.
15. GRABILL, C., A.C. SILVA, S.S. SMITH *et al*. 2003. MRI detection of ferritin iron overload and associated neuronal pathology in iron regulatory protein-2 knockout mice. Brain Res. **971:** 95–106.
16. MARTIN, L.J., N.A. AL-ABDULLA, A.M. BRAMBRINK *et al*. 1998. Neurodegeneration in excitotoxicity, global cerebral ischemia, and target deprivation: a perspective on the contributions of apoptosis and necrosis. Brain Res. Bull. **46:** 281–309.
17. ARMSTRONG, R.A., P.L. LANTOS & N.J. CAIRNS. 2002. Spatial patterns of the vacuolation in subcortical white matter in sporadic Creutzfeldt-Jakob disease (sCJD). Clin. Neuropathol. **21:** 284–288.
18. HE, L., X.Y. LU, A.F. JOLLY *et al*. 2003. Spongiform degeneration in mahoganoid mutant mice. Science **299:** 710–712.
19. ROUAULT, T.A. 2001. Iron on the brain. Nat. Genet. **28:** 299–300.

20. KAUR, D., F. YANTIRI, S. RAJAGOPALAN *et al.* 2003. Genetic or pharmacological iron chelation prevents MPTP-induced neurotoxicity *in vivo*: a novel therapy for Parkinson's disease. Neuron **37:** 899–909.
21. LOPACHIN, R.M., C.D. BALABAN & J.F. ROSS. 2003. Acrylamide axonopathy revisited. Toxicol. Appl. Pharmacol. **188:** 135–153.
22. RAFF, M.C., A.V. WHITMORE & J.T. FINN. 2002. Axonal self-destruction and neurodegeneration. Science **296:** 868–871.
23. GILL, S.S., N.K. PATEL, G.R. HOTTON *et al*. 2003. Direct brain infusion of glial cell line–derived neurotrophic factor in Parkinson disease. Nat. Med. **9:** 589–595.